방광 내 주입용 폴록사머 407 하이드로젤 제형의 고분자 첨가제 스크리닝: 기계적 성질, 젤 형성 능력 및 약물 방출 평가

양희망# · 원용훈# · 윤호엽 · 김창현 · 구윤태 · 장인호* · 최영욱†

중앙대학교 약학대학, *중앙대학교 의과대학

(2020년 6월 16일 접수, 2020년 7월 28일 수정, 2020년 8월 4일 채택)

Screening of Polymer Additives in Poloxamer 407 Hydrogel Formulations for Intravesical Instillation: Evaluation of Mechanical Properties, Gel-forming Capacity, and Drug Release

Hee Mang Yang#, Yong Hoon Won#, Ho Yub Yoon, Chang Hyun Kim, Yoon Tae Goo, In Ho Chang*, and Young Wook Choi†

College of Pharmacy, Chung-Ang University, 84 Heuksuk-ro, Dongjak-gu, Seoul 06974, Korea
*College of Medicine, Chung-Ang University, 84, Heuksuk-ro, Dongjak-gu, Seoul 06974, Korea

(Received June 16, 2020; Revised July 28, 2020; Accepted August 4, 2020)

초록: 폴록사머 407(PLX) 하이드로젤은 방광 내 주입을 위한 전달 시스템으로 사용되고 있지만, 젤의 강도가 충분하지 않다는 한계가 있다. 하이드로젤의 점도 및 강도를 조절하기 위해, 다양한 고분자 첨가제를 선별하였다. 점도의 변화는 고분자량 히알루론산(HHA; 33.524 Pa·s) > 히드록시프로필메틸셀룰로스 > 키토산 > 저분자량 HA > 알긴산 > 카보폴(24.332 Pa·s) 순서로 관찰되었다. 고분자 첨가는 PLX 하이드로젤의 열 가역적 특성을 변화시키지 않았으며, 젤화 온도(21.0-25.3 °C) 및 젤화 시간(17.28-28.32초)을 나타내었다. 수용성인 젬시타빈을 탑재한 채로 방광 시뮬레이션 모델을 통해 젤 침식 및 약물 방출을 조사하였다. 4회 반복시험 후 남아있는 양을 관찰하였을 때 HHA 첨가 하이드로젤 및 PLX 하이드로젤이 각각 74.6% 및 57.8%로 나타났으며, 약물 방출은 확산 및 침식으로 제어되었다. 따라서 HHA 첨가 하이드로젤은 방광 내 주입을 위한 유망한 시스템으로 판단된다.

Abstract: Poloxamer 407 (PLX) hydrogel has been used as a drug delivery system for intravesical instillation, but it has a limitation of insufficient gel strength. Here, to modulate the viscosity and strength of hydrogel, various polymers were screened. Their effect on viscosity decreased in the following order: high molecular-weight hyaluronic acid (HHA; 33.524 Pa·s) > hydroxypropyl methylcellulose > chitosan > low-molecular weight HA > sodium alginate > carbopol (24.332 Pa·s). Polymer addition hardly altered the thermo-reversible property of hydrogels; the gelation temperature was 21.0–25.3 °C and gelation time was 17.28–28.32 s. With gemcitabine as a water-soluble ingredient, gel erosion and drug release were examined using an *in vitro* bladder simulation model. After four repeated cycles of filling and emptying, the remaining fraction of HHA-added hydrogel and PLX hydrogel was 74.6% and 57.8%, respectively. Furthermore, drug release was diffusion- and erosion-controlled. Thus, HHA-added hydrogel is a promising system for intravesical instillation.

Keywords: poloxamer 407, hydrogel, gemcitabine, hyaluronic acid, intravesical instillation.

Introduction

Bladder cancer, one of the most common cancers worldwide,[1] is a heterogeneous disease, and 70% of patients have a superficial tumor with a low risk of death and 30% have a life-threatening muscle-invasive tumor.[2] The standard treatments for bladder cancer include radiotherapy, radical cystectomy, immunotherapy, and chemotherapy. Various chemotherapeutic agents such as paclitaxel, doxorubicin, and cisplatin are used as drugs of choice for bladder cancer treatment. Recently, gemcitabine (GEM) has been commonly used in combination or adjuvant chemotherapy for bladder cancer.[3] However, these agents generally fail to reach the therapeutic range when injected intravenously. This limitation can be overcome by two

strategies, namely, dose increment and intravesical instillation. Because the former leads to systemic adverse effects, the latter is a better option to treat bladder cancer. However, intravesical instillation of a drug into the bladder using a catheter has a limitation of dilution by urine and washout during urination. These challenges can be overcome by employing *in-situ* gelling systems with sol–gel transition property.

A hydrogel is a hydrophilic polymer network that contains a large amount of water while maintaining its gel form.[4,5] It possesses several advantages such as diverse drug-incorporating capacity and *in-situ* sol–gel transition after instillation in the body cavity. The typical mechanism of sol–gel transition includes temperature- or pH-induced transition.[6,7] Thermo-sensitive hydrogels exist in the hard-to-flow phase at the body temperature of 37 °C or free-flowing phase at low temperature (e.g., 4 °C).

Poloxamers, known as ABA-type triblock copolymers, consist of blocks of ethylene oxide (EO) and propylene oxide (PO) units.[8] One of the most important characteristics of poloxamer is thermo-sensitiveness. Poloxamers have a unique sol–gel transition temperature, at which they are in a flowable fluid form, termed as sol. As the temperature increases, the poloxamer molecules aggregate to form micelles, owing to the dehydration of the hydrophobic PO blocks. The packing of these micelles, with the poly PO core and poly EO outer shell, contribute to gelation, resulting in an un-flowable fluid, termed as gel.[9,10] Because of these characteristics, poloxamer hydrogel has advantages as a delivery system for intravesical instillation; it is also less toxic. Despite these merits, hydrogels composed of only poloxamers do not have sufficient gel strength.

The addition of various excipients can modulate the viscosity and strength of hydrogels.[11] Neutral (carbopol, hydroxypropyl methylcellulose, and hyaluronic acid), anionic (alginate, sodium carboxymethylcellulose, and methacrylic acid copolymers), and cationic (chitosan, chitin, and polyethylenimine) biocompatible polymers are commonly used. The interactions between polymeric additives and poloxamers are known to change the gel microstructure and rheological and mechanical properties. These infrastructural and physicochemical changes could affect the gel-forming capacity and the movement of drugs entrapped within the gel structure, thereby changing the gel matrix erosion and drug release characteristics.[12-16]

In the present study, the strength of hydrogel was modulated by adding selective polymers such as polysaccharide, cellulose derivatives and carbohydrates. Mechanical properties of the modulated hydrogels were evaluated in terms of viscosity, hardness, compressibility, adhesiveness, and cohesiveness. Gel-forming capacity, in terms of gelation temperature and gelation time, was compared among the hydrogels. Moreover, by adopting an *in vitro* bladder simulation model, gel erosion and GEM release from the hydrogels were investigated. We expect that these characteristics would be favorable to develop a suitable drug delivery system for intravesical instillation in bladder cancer treatment.

Experimental

Materials. Poloxamer 407 (PLX) was supplied by BASF Laboratories (Wyandotte, MI, USA). Chitosan from crab shells (CS; >400 mPa·s at 1% in acetic acid at 20 °C, ≥75% deacetylated), hydroxypropyl methylcellulose (HPMC; <26 kDa, 80–120 cps at 2% in water at 20 °C), sodium alginate (ALG; 15–25 cps at 1% in water) and phosphate-buffered saline (PBS) tablet were purchased from Sigma-Aldrich (St. Louis, MO, USA). Carbopol® 934NF (CP) was purchased from Lubrizol (Cleveland, OH, USA). Low-molecular weight hyaluronic acid from cockscomb (LHA; 5–150 kDa) was purchased from TCI (Toshima, Kita-ku, Tokyo, Japan). High-molecular weight hyaluronic acid (HHA; ≥1000 kDa) was purchased from Thermo Fisher Scientific (Ward Hill, MA, USA). Acetonitrile was purchased from J. T. Baker (Phillipsburg, NJ, USA). GEM was provided by Shin Poong Pharm. Co., Ltd. (Gangnam, Seoul, Korea). All other solvents used were of analytical grade.

Preparation of PLX Hydrogel Samples. Thermo-reversible PLX hydrogel was prepared using the cold technique.[17] To prepare PLX hydrogel without additives (reference sample), 20 w/v% PLX was added to distilled water and stirred using a magnetic stirrer overnight in a refrigerator (CLG-650; Jeio Tech, Daejeon, Korea) at 4 °C until the PLX granules were completely dissolved. Polymer-added test samples were prepared by adding the respective polymers (CS, ALG, HPMC, CP, LHA, and HHA) to the PLX solution at 1 w/v% concentration, and then stirred overnight at 4 °C until a clear solution was obtained. GEM was loaded into different hydrogels (1.5 mg/mL) and completely dissolved by stirring overnight under the same conditions.

Visual Observation of the Thermo-reversible Property. Five milliliters of different hydrogels was loaded into transparent vials and stored at 4 °C (in a refrigerator) and 37 °C (in a temperature-controlled water bath, WB-11; Daihan Scientific, Wonju, Korea). The vials were then tilted, and the degree

of flowability was visually observed to confirm the thermo-reversible transition from sol to gel.

Evaluation of Mechanical Properties. The textural properties of different hydrogels were measured using the TA-XT Express (Stable Micro System Ltd., Surrey, UK). While avoiding air entrapment and making the upper surface smooth, 25 mL of samples was filled in 50 mL beakers. When each sample changes to the gel state at 37 °C, a 20 mm (diameter) probe was inserted into the sample. The test speed rate, distance (depth of insertion), and trigger force were set to 0.5 mm/s, 5 mm, and 1 g, respectively.[18] The mechanical parameters of hydrogels, such as hardness, compressibility, adhesiveness, and cohesiveness, were determined from the force versus time plot. The maximum force reflects the hardness of hydrogel, and it is defined as the force required to deform the sample. The area of downward movement of the probe shows the compressibility of hydrogel, whereas the area of upward movement of the probe shows the adhesiveness of hydrogel. The proportional force of the first downward movement to the second downward movement of the probe can be defined as cohesiveness. Separately, the viscosity of hydrogels was measured using the Advanced Rheometric Expansion System (ARES; Rheometric Scientific Inc., London, UK). In the gel state of the samples, 2 mL of hydrogel was loaded into 25 mm parallel plates of the ARES. With a single steady rate of 8 h⁻¹ and 1 mm gap, the viscosity of each sample was measured while maintaining 37 °C.[19] The texture analysis and viscosity measurement were performed in triplicates and the values were averaged.

Measurement of Gelation Temperature and Gelation Time. The gelation temperature and gelation time were measured using the test-tube inversion method.[20,21] An aliquot (1 mL) of the sample was instilled into 5 mL test tubes (11 mm diameter) at 4 °C, as the sol phase. The prepared test tubes containing hydrogel were placed in a temperature-controlled water bath and the temperature was gradually increased at the rate of 1 °C/min from 4 to 37 °C. The temperature at which the sample does not flow for 30 s when the test-tube is inverted is the gelation temperature. Separately, 1 mL of the sample was injected into a 5 mL test tube at 4 °C as the sol phase, and immediately, the test tube was placed in a water bath of 37 °C; then, the gelation time was checked every 5 s until the sample was not flowable, as the gel phase. The measurements were performed in triplicate.

In Vitro **Gel Erosion and Drug Release Study.** Based on a previous study,[22] as illustrated in Figure 1, an *in vitro* urinary bladder simulation model was adopted to examine gel erosion and drug release characteristics. Gel erosion was evaluated using the gravimetric method as previously reported.[22] Briefly, 12 mL of hydrogel samples was instilled into an empty 250 mL round-bottom flask at a constant temperature of 37 °C using a water bath and the total weight (W_0) was recorded. Subsequently, PBS medium maintained at 37 °C was added into the flask at a rate of 2 mL/min through a peristaltic pump (BT100-2J; Longer Precision Pump Co., Ltd., Hebei, China). After peristalsis for 2 h, the supernatant solution was discarded and the residual weight of the flask (W_t) was recorded. Fresh PBS medium was infused at the same rate under the same conditions, and the process was repeated four times. The remaining fraction of hydrogels (%) was calculated using the following equation: (W_t/W_0) × 100. The measurements were performed in triplicate.
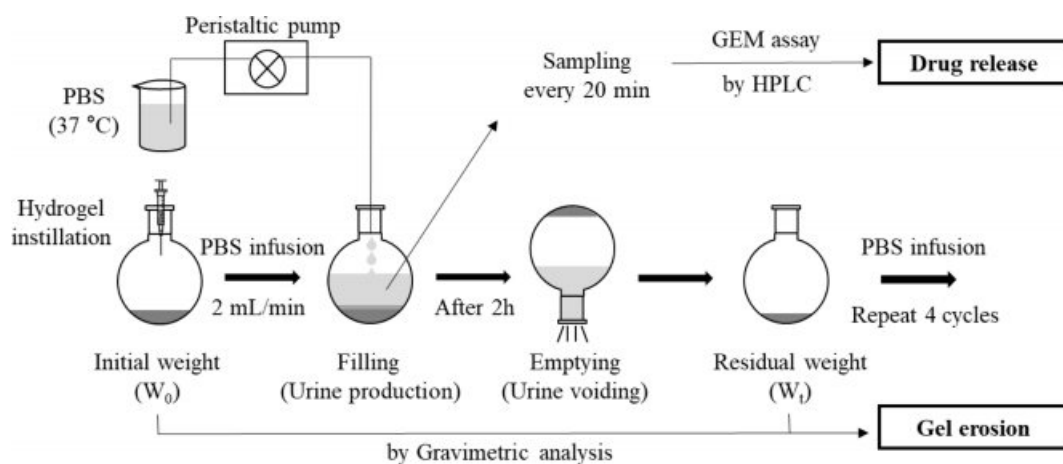

Figure 1. Illustration of the *in vitro* bladder simulation model for drug release and gel erosion study. Filling and emptying cycles repeated every 2 h.

Simultaneously, drug release from the hydrogel was investigated by determining the GEM concentration in the PBS solution by high-performance liquid chromatography (HPLC). Briefly, 0.5 mL of the supernatant solution was sampled at every 20 min and an equivalent volume of fresh PBS was replenished to maintain the constant volume of release medium.[16] After filtration using a 0.45 μm polyvinylidene fluoride filter (PVDF; Whatman International Ltd., Maidstone, UK), each sample was subjected to HPLC assay of GEM. The HPLC system consisted of a pump (W2690/5; Waters Corporation, Milford, MA, USA), an ultraviolet detector (W2489; Waters Corporation, Milford, MA, USA), a data station (Empower 3; Waters, Milford, MA, USA), and a ZORBAX ODS C18 column (4.6 mm ID × 150 mm; Agilent, CA, USA). The mobile phase was composed of water and acetonitrile (9:1, v/v) and the column temperature was 25 °C. The flow rate was 1.0 mL/min, and the injection volume was 20 μL. GEM was detected at a wavelength of 275 nm. The drug release tests were conducted in triplicate.

Kinetics Analysis of GEM Release. To investigate the mechanism of drug release from the prepared hydrogels, different mathematical kinetic models were employed. The results of the drug release test were fit to the zero-order kinetics (eq. (1)), first-order kinetics (eq. (2)), Higuchi kinetics (eq. (3)), Hixson–Crowell equation (eq. (4)), and Ritger–Peppas equation (eq. (5)) as follows:[23,24]

$$M_t/M_\infty = K_0 t \tag{1}$$

$$M_t/M_\infty = 1 - e^{-K_1 t} \tag{2}$$

$$M_t/M_\infty = K_H t^{1/2} \tag{3}$$

$$\sqrt[3]{M_\infty} - \sqrt[3]{M_t} = K_{HC} t \tag{4}$$

$$M_t/M_\infty = K_{RP} t^n \tag{5}$$

where M_t/M_∞ is the fraction of drug released at time t; M_t is the amount of the drug released at time t; M_∞ is the initial amount of drug in the hydrogel; n is the diffusion exponent; and K_0, K_1, K_H, K_{HC}, and K_{RP} are the rate constants for zero-order, first-order, Higuchi, Hixson–Crowell, and Ritger–Peppas equations, respectively.

Statistical Analysis. All data are expressed as mean ± standard deviation (n ≥ 3). Significant differences were determined using the Student's *t*-test, and the results with a *p*-value <0.05 were considered statically significant.

Results and Discussion

Thermo-reversible Property of the Prepared Hydrogels. Various PLX hydrogels were successfully prepared using the cold technique in the presence or absence of polymeric additives. PLX and the additives were completely dissolved in water to form a clear solution at 4 °C. Most PLX hydrogels were colorless and transparent, and the addition of CS and CP resulted in an opaque hydrogel and ALG resulted in a pale-yellow hydrogel. As shown in Figure 2, all prepared hydrogels exhibited the thermo-reversible property, that is, free-flowing at 4 °C but hard-to-flow at 37 °C. Thus, we confirmed that these behaviors are reversible and that all the selected additives do not alter the thermo-reversible property of PLX hydrogel.

Mechanical Properties of the Prepared Hydrogels. The viscosity of hydrogels was measured based on the dependence of non-Newtonian fluids on shear stress and shear rate, according to the rheological measurements. The viscosity of the PLX hydrogel was 29.453 Pa·s. The viscosity of different hydrogels decreased in the following order: HHA > HPMC > CS > plain PLX > LHA > ALG > CP (Table 1).

The texture analysis could provide an overview of the mechanical properties of hydrogels, namely, hardness, compressibility, adhesiveness, and cohesiveness. The hardness and compressibility of the PLX hydrogel were 28.524 g and 236.012 g·s, respectively. The addition of HPMC, ALG, CS, and HHA increased the hardness to more than 50 g, whereas
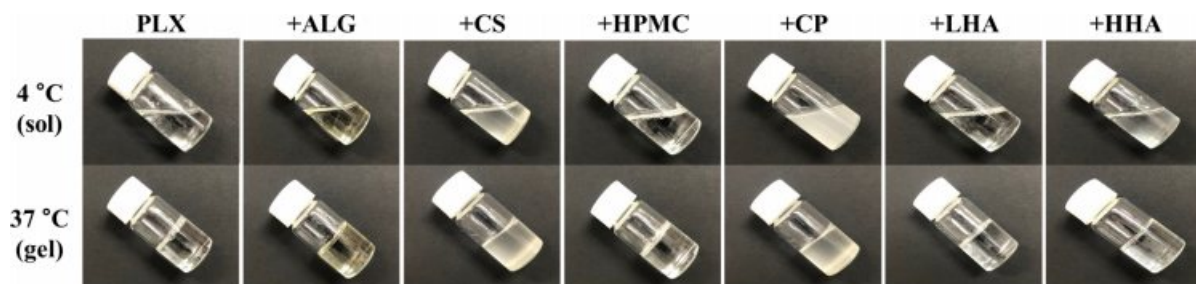

Figure 2. Observation of thermo-sensitive phase transition.

Table 1. Mechanical Properties of Various Hydrogels

	Viscosity (Pa·s)	Hardness (g)	Compressibility (g·s)	Adhesiveness (g·s)	Cohesiveness (unitless)
PLX	29.45 ± 0.823	28.52 ± 0.011	236.01 ± 0.009	141.60 ± 0.004	0.55 ± 0.001
+ALG	26.94 ± 0.510	50.41 ± 0.010	332.18 ± 0.006	355.31 ± 0.007	1.16 ± 0.005
+CS	29.94 ± 0.041	59.28 ± 0.004	161.91 ± 0.002	304.78 ± 0.002	1.78 ± 0.065
+HPMC	32.85 ± 0.391	60.50 ± 0.040	455.20 ± 0.001	468.84 ± 0.006	1.03 ± 0.002
+CP	24.33 ± 0.804	11.17 ± 0.027	97.70 ± 0.017	140.34 ± 0.004	0.76 ± 0.007
+LHA	29.28 ± 0.334	15.94 ± 0.049	144.70 ± 0.019	186.07 ± 0.004	0.75 ± 0.005
+HHA	33.52 ± 1.073	52.02 ± 0.024	397.70 ± 0.007	377.30 ± 0.003	1.00 ± 0.007

Values are presented as mean ± SD (n = 3).

the addition of CP and LHA decreased the value to extremely low levels, 11.166 and 15.940 g, respectively. Similarly, HPMC addition resulted in the highest compressibility of 455.201 g·s, which was approximately two-fold higher than that of the PLX hydrogel. The addition of ALG and HHA also increased the compressibility, whereas the addition of CS, CP, and LHA decreased it to the range of 97.7–161.9 g·s. Overall, CP and LHA resulted in lower hardness and compressibility than the other additives, indicating the ease of instillation and good spreadability of hydrogels with these polymers.

The adhesiveness and cohesiveness of the PLX hydrogel were 141.595 g·s and 0.551, respectively. The addition of HPMC significantly increased the adhesiveness by more than three-fold (468.838 g·s). The other additives also increased the adhesiveness (g·s) in the following order: HHA (377.3) > ALG (355.3) > CS (304.8) > LHA (186.1) > CP (140.3). Similarly, the addition of polymers resulted in a 1.4–3.2-fold increase in cohesiveness. Specifically, the addition of CS resulted in the highest level cohesiveness of 1.780, whereas the addition of LHA yielded the lowest (0.746). These results suggest that HPMC and HHA were preferable among the additives studied.

Comparison of Gel-forming Capacity. The gel-forming capacity of different hydrogels was compared in terms of gelation temperature and gelation time (Table 2). These parameters were adopted to estimate the capacity for long-term retention and rapid gel formation of hydrogel after instillation into the bladder. The PLX hydrogel presented the highest gelation temperature of 25.3 °C, whereas HHA-added hydrogel presented the lowest temperature of 21.0 °C. Thus, in terms of gelation temperature, all prepared hydrogels should be cooled before instillation.

On the contrary, the PLX hydrogel had the longest gelation

Table 2. Gel-forming Capacity of Various Hydrogels

	Gelation temperature (°C)	Gelation time (s)
PLX	25.3 ± 0.47	28.3 ± 0.29
+ALG	24.7 ± 0.47	23.1 ± 0.67
+CS	24.3 ± 1.25	26.9 ± 0.11
+HPMC	24.6 ± 1.89	25.9 ± 0.27
+CP	23.3 ± 1.25	21.3 ± 1.14
+LHA	23.0 ± 0.82	27.7 ± 0.8
+HHA	21.0 ± 0.82	17.3 ± 0.08

Values are presented as mean ± SD (n = 3).

time (28.32 s), whereas HHA-added hydrogel had the shortest time (17.28 s). As the gelation time of the other hydrogels was in the range of 17–30 s, we consider that all the formulations were injectable to the bladder without any difficulties including dilution by urine and/or obstruction of catheter needle.

In Vitro Gel Erosion. The gel erosion profiles were examined using an *in vitro* bladder simulation model as reported previously.[25,26] In this model, to mimic physiological urine production and urine voiding, PBS medium was infused into a gel-loaded flask at 2 mL/min, and after 2 h, the whole medium was discarded; this cycle was repeated four times, and the gravimetric analysis based on weight loss in every cycle was applied to obtain the remaining fraction of hydrogels.

The remaining fraction (%) over four repeated cycles of filling–emptying was plotted against time (Figure 3(a)). Overall, the remaining fraction of hydrogels linearly reduced with time, indicating that the erosion followed zero-order kinetics. After the first cycle (2 h), approximately 5–10% erosion was observed in most hydrogels, revealing no significant difference between the PLX hydrogel and polymer-added hydrogels. However,
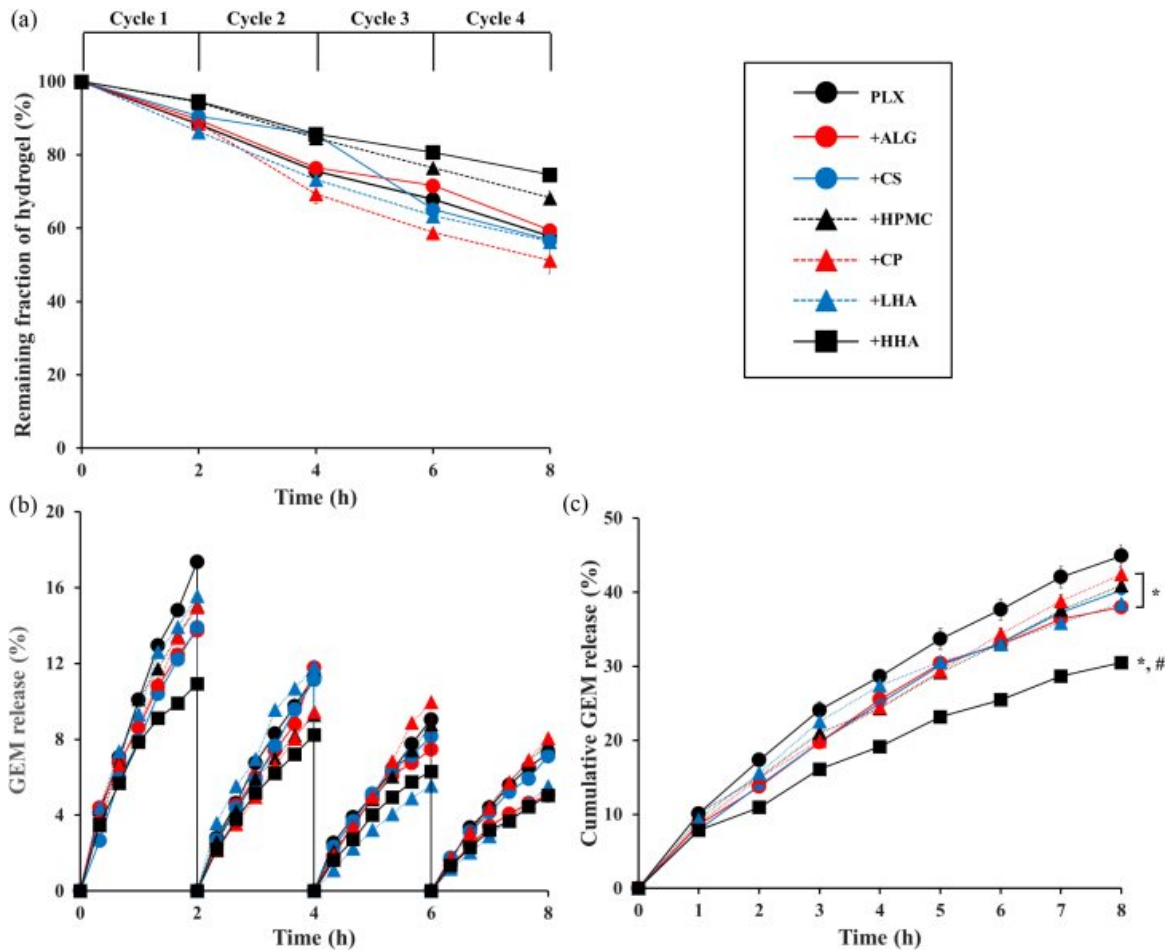
Figure 3. Results of *in vitro* gel erosion and gemcitabine (GEM) release. (a) Plot of remaining fraction of hydrogel (%) *versus* time for four repeated cycles. (b) Plot of GEM release (%) *versus* time for every cycle. (c) Plot of cumulative GEM release (%) *versus* time. Significantly different at $p<0.05$: *versus* PLX hydrogel; #versus other polymer-added hydrogel. Values are presented as mean ± SD (n=3).

thereafter, differences in the formulations manifested, with the highest erosion in CP-added hydrogel and the lowest erosion in HHA-added hydrogel. After four cycles (8 h), erosion in the remaining fraction (%) of hydrogels decreased in the order of HHA-added (74.6) > HPMC-added (68.3) > ALG-added (59.4) > PLX (57.8) > CS-added (56.7) > LHA-added (56.4) > CP-added (51.3).

GEM Release Profile. The profiles of GEM release were examined every 20 min over the four repeated cycles. Figure 3(b) represents the plot of the amount of GEM released *versus* time in every cycle. In the first cycle (2 h), the PLX hydrogel showed a higher release than other polymer-added hydrogels, of 17.4%, whereas HHA-added hydrogel showed the most sustained release pattern (10.9%) and the other polymer-added hydrogels showed an intermediate release pattern between the above percentages. Furthermore, the degree of GEM release

was gradually reduced with filling–emptying cycles. The degree of drug release for most hydrogels was maintained in the same order, except for the CP-added and LHA-added hydrogels.

For further comparison, the cycle-based plot was converted to the cumulative amount plot of GEM release *versus* time (Figure 3(c)). At 1 h, no significant differences were found among the hydrogels, showing approximately 10% GEM release. However, at the end of the first cycle (2 h), polymer-dependent differences were observed, and the difference increased with time. After 5 h, compared with the PLX hydrogel, all polymer-added hydrogels showed a significant difference ($p<0.05$). In particular, after 3 h, HHA-added hydrogel showed a significant difference relative to both PLX hydrogel and other polymer-added hydrogels. After four cycles (8 h), the cumulative GEM release (%) decreased in the following order: PLX (44.9) > CP-added (42.4) > HPMC-added (40.9) >

CS-added (40.3) > LHA-added (38.5) > ALG-added (38.0) > HHA-added (30.5). These results suggest that among the polymeric additives used in this study, HHA was superior in terms of sustaining the release of GEM.

We prepared thermo-reversible PLX hydrogel formulations to screen for those with prolonged retention time and sustained drug release in the bladder cavity. PLX and the selected additives are biocompatible, and they have been widely used in the pharmaceutical industry owing to their low toxicity. Based on a previous study, the concentration of PLX was set to 20 w/v%, at which sensitive sol-to-gel transition and sufficient consistency in the gel state can be observed.[25] Although the content of polymer used in hydrogel formulations has been shown to vary from 0.1 to 4 w/v%,[27] in this study, the content of polymeric additives was 1 w/v% for relative comparison. The addition of polymers did not affect the thermo-reversible property of PLX hydrogel, even though the gelation temperature was slightly reduced. Gelation temperature is the minimum temperature at which thermo-reversible hydrogel is in the gel state. To enable phase transition in the bladder cavity after instillation, the gelation temperature should be below the physiological body temperature, that is, 37 °C. Gelation time is the time needed for sol-to-gel transition, which should be within a minute to avoid unexpected dilution by urine. However, if this gelation time is too short (i.e., within several seconds), the hydrogel may obstruct the catheter needle during intravesical instillation. In the present study, the HHA-added hydrogel presented the lowest gelation temperature (21.0 °C) and shortest gelation time (17.28 s), which indicate its potential to undergo gelation after instillation in the bladder and rapidly form a gel. These results are consistent with those of previous studies.[25,28]

Here, texture profile and viscosity analyses are proposed as an appropriate tool to characterize the hydrogel system. Depending on the type of polymer, the mechanical properties, such as viscosity, hardness, compressibility, adhesiveness, and cohesiveness, of the hydrogels changed. Viscosity signifies the molecular movement of viscoelastic materials, and different viscosities imply differences in the molecular structure, reflecting intermolecular interaction.[29,30] Furthermore, viscosity also indicates the ease at which a hydrogel can be injected using a syringe, as a low viscosity is required to reduce the force required to instill.[31] Hardness, measured by the peak of force needed to achieve deformation, reflects the ease of instillation; a low value represents ease of administration. Compressibility, defined by the work needed to deform the hydrogel during compression, indicates the ease of spreadability in the inner bladder cavity. Adhesiveness, measured by the work needed to overcome attractive forces between the hydrogel surface and probe, is a comparative measure of the adhesive ability of hydrogels in the bladder cavity and a good indicator of retention in the bladder.[32] Cohesiveness, defined by the ratio of force of the second deformation to that of the first deformation, is related to the structural recovery of hydrogel after application in the bladder cavity.[33]

Selection of appropriate polymer additives is a crucial aspect in modulating the properties of PLX hydrogel, especially in terms of gel erosion and drug release. CS is a biodegradable natural polymer.[34] By blending CS with PLX hydrogel, drug release rate can be reduced and residence time in the administration site can be extended.[12,35,36] This is because of the interpenetration of CS into the PLX gel network, which decreases the rate of water penetration into the hydrogel. The slower rate of drug release from CS-added hydrogel is also related to the tortuosity of microchannels for drug diffusion, which results in a longer time to release the drug. These characteristics are related to the molecular weight and concentration of CS.[37-39]

ALG is a relatively strong mucoadhesive anionic polymer.[40] The physical mixing of ALG with PLX is reported to increase retention time and sustain drug release from the hydrogel system.[11] This phenomenon is caused by the formation of crosslinks between ALG and PLX. The water molecules may function as a cross-linking agent to create hydrogen bonds between the carboxyl groups of ALG and the ether group of PLX, which may form a three-dimensional network. Therefore, this interaction affects the sol–gel transition temperature and sustained release behavior.[13,35] In addition, the pKa of a drug molecule could be an influencing factor because ALG is an anionic polymer.[41]

HPMC is a cellulose derivative. Because of different molecular weights, they have a wide range of viscosity, adsorptive activities, and osmotic properties. Because of these characteristics, HPMC is used as a component of various gels including dermatological and ophthalmological gels.[42] The sustained release property of HPMC-added hydrogel has been explained by a previous study,[43] which described that the viscosity of hydrogels increased with the use of HPMC owing to its ability to bind the poly EO chains, increasing the entanglement of the adjacent molecules. Thereby, the polymer additives decrease the initial burst and prolong drug release. Similarly, Zhang et al. reported that HPMC swells in solution and forms disordered physical networks. Thus, the extensive hydrogen bonds and the molecule entanglement could form tightly orientated

hydrogel structure, resulting in delayed drug diffusion and gel dissolution.[44]

CP, also known as a carbomer, is an acrylic acid derivative, which is widely used as a gel-forming agent in soft medicinal formulations. There are various brands of CP, classified according to the rate of gel formation, transparency of gels, and ability to suspend and emulsify.[42] Moreover, they have excellent mucoadhesive properties in ocular delivery and sustained drug release profile when mixed with PLX.[16] The reasons of the sustained drug release profile of CP-added hydrogel have been explained by a previous study, which reported that CP can form a polymer complex with PLX by hydrogen bonding, subsequently reinforcing the network structure and slow relaxation and hydration of the polymer matrix.[45]

HA is a natural biodegradable polysaccharide.[46] It is used alone or in combination with others and is mainly used for joint lubrication and ocular delivery.[47] It is known that HA, when mixed with PLX hydrogel, increases gel strength and decreases gel network porosity. In addition, Mayol *et al.* reported that HAs of different molecular weights vary in rheological behavior when mixed with PLX hydrogel.[48] The sustained release property of the HA molecules is because they can interact with PLX micelles via hydrogen bonding, thus reinforcing the structure of micelles and mechanical properties of hydrogel.[48] Moreover, the possibility of interaction between HHA random coils and PLX micelles increases aggregation relative to that by PLX-only micelles or PLX-LHA micelles.[48] The micelle movement is increasingly hampered as PLX gelation progresses. A similar study showed that the addition of HHA resulted in a sustained release, while preventing the initial burst.[49] The reason for this behavior is ascribed to the closely packed inter-micellar structure by the addition of HHA. Furthermore, the highly packed supramolecular structure reduces the diffusion coefficients of HHA-added hydrogel, which could result in prolonged drug release. These findings

are consistent with our results, in which HHA-added hydrogel showed better sustained GEM release behavior than the other polymer-added hydrogels.

Mathematical kinetic models are an important tool to evaluate the drug release process. They can be used to evaluate some important physical parameters and have recourse for model fitting experimental release data.[50] By curve fitting to the different kinetics, such as the zero-order, first-order, Higuchi, Hixson–Crowell, and Ritger–Peppas equations, correlation coefficient (R^2) of all formulations were obtained. All R^2 values were greater than 0.9 (Table 3), indicating a good linearity. Among various kinetic models, the Ritger–Peppas model was the best fit with the highest R^2 value. Specifically, this model is useful to characterize polymeric systems, in which the release mechanism is not fully understood or complex.[50] In addition, the Ritger–Peppas model provides the value of diffusion exponent (n), which better determines the mechanism of a drug diffusion from a matrix system whether the diffusion is Fickian or non-Fickian. As shown in Table 3, all formulations presented values in the range of 0.6835–0.8153, indicating non-Fickian diffusion. This type of anomalous release is governed by swelling and diffusion. The slow rearrangement of polymeric chains (swelling and finally erosion) and simultaneous diffusion induce the time-dependent anomalous effects.[51] Therefore, all additives may follow the erosion–diffusion mechanism. Thus, both hydrogel erosion and GEM diffusion are important processes in GEM release from the hydrogels tested in this study.

Furthermore, we investigated the correlations between gel erosion and drug release. The PLX hydrogel and HHA-added hydrogel were selected as representatives for the analysis, and the cumulative amount of GEM release (%) was plotted against gel erosion (%). For plotting, the values at specific time points were obtained using the regression equations of the Ritger–Peppas model (GEM release) and zero-order kinetics (gel

Table 3. Comparison of Correlation Coefficients (R²) in Various Mathematical Kinetic Models

	PLX	+ALG	+CS	+HPMC	+CP	+LHA	+HHA
Zero-order	0.9748	0.9727	0.9814	0.9841	0.9912	0.9441	0.9788
First-order	0.9936	0.987	0.9948	0.9957	0.9982	0.9689	0.99
Higuchi	0.9856	0.9785	0.9781	0.9818	0.9728	0.9885	0.9835
Hixson–Crowell	0.9888	0.983	0.9914	0.9931	0.9972	0.9615	0.9868
Ritger–Peppas	0.9967	0.9955	0.9955	0.9986	0.9992	0.9905	0.9974
n value*	0.7476	0.7194	0.8153	0.7073	0.7437	0.6835	0.6896

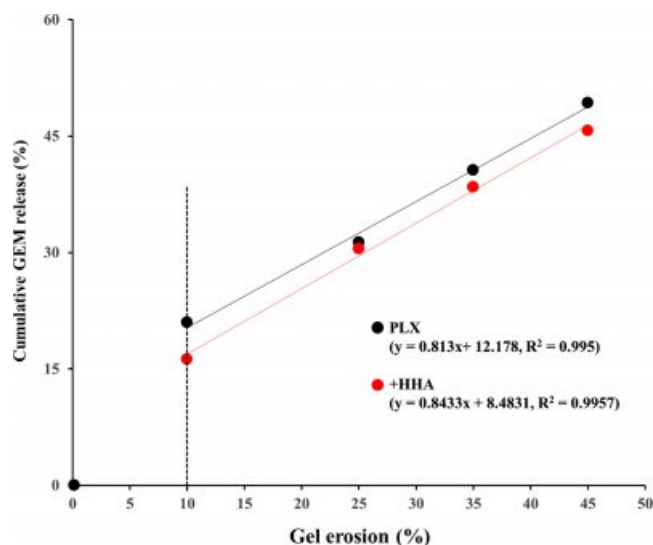*Diffusion exponent related to the Ritger–Peppas model.

Figure 4. Relationship between cumulative GEM release (%) and gel erosion (%) for plain PLX and HHA-added hydrogel. Values at specific time points were calculated using the regression equations of the Ritger–Peppas model (GEM release) and zero-order kinetics (gel erosion).

erosion). Both PLX and HHA-added hydrogels showed a similar pattern (Figure 4), indicating negligible influence of polymer addition on this correlation. Until 10% erosion, there was an initial burst, which can be attributed to the leakage of drug during gel formation and/or rapid diffusion of drug molecules adjacent to bulk front. The addition of HHA decreased the level of initial burst. Except at this period, correlations between gel erosion and GEM release were well-established for both hydrogels, with the R^2 values of 0.9950 and 0.9957 for PLX hydrogel and HHA-added hydrogel, respectively. Moreover, the slope of regression equations was close to unity, implying GEM release proportional to gel erosion. Several studies have described the erosion-controlled release kinetics of hydrogels.[26] Other factors such as molecular size and hydrophilicity are also important. If a drug molecule is hydrophobic, drug release is mainly governed by gel erosion. However, as GEM, with a molecular weight of 263 Da, is water soluble, drug release is governed by both gel erosion and molecular diffusion. Therefore, we expect that these hydrogels, preferably HHA-added hydrogels, are good candidates for developing an in-situ gelling system to increase drug exposure in bladder cancer treatment.

Conclusions

PLX-based hydrogels with or without polymer additives

were successfully formulated while maintaining its thermo-reversible property. With excellent gel-forming capacity, the hydrogels revealed acceptable mechanical properties in terms of viscosity, gel strength, and adhesiveness. Drug release was diffusion and erosion controlled. Specifically, HHA-added hydrogel is a promising system for intravesical instillation in the treatment of bladder cancer. However, further *in vivo* assessments are still needed.

References

1. S. Antoni, J. Ferlay, I. Soerjomataram, A. Znaor, A. Jemal, and F. Bray, *Eur. Urol.*, **71**, 96 (2017).
2. H. Rubben, H. Lutzeyer, N. Fischer, F. Deutz, W. Lagrange, and G. Giani, *J. Urol.*, **139**, 283 (1988).
3. D. S. Kaufman, W. U. Shipley, and A. S. Feldman, *Lancet*, **374**, 239 (2009).
4. M. K. Nguyen and D. S. Lee, *Macromol. Biosci.*, **10**, 563 (2010).
5. A. S. Hoffman, *Adv. Drug Deliv. Rev.*, **54**, 3 (2012).
6. C. He, S. W. Kim, and D. S. Lee, *J. Control. Release*, **127**, 189 (2008).
7. L. Yu and J. Ding, *Chem. Soc. Rev.*, **37**, 1473 (2008).
8. A. V. Kabanov, E. V. Batrakova, and V. Y. Alakhov, *J. Control. Release*, **82**, 189 (2002).
9. J. Juhasz, V. Lenaerts, P. Raymond, and H. Ong, *Biomaterials*, **10**, 265 (1989).
10. G. Dumortier, J. L. Grossiord, F. Agnely, and J. C. Chaumeil, *Pharm. Res.*, **23**, 2709 (2006).
11. H. Abdeltawab, D. Scirskis, and M. Sharma, *Expert. Opin. Drug Deliv.*, **17**, 495 (2020).
12. A. C. S. Akkari, J. Z. B. Papini, G. K. Garcia, K. K. Margareth, D. Franco, L. P. Cavalcanti, A. Gasperini, M. I. Alkschbirs, F. Yokaichyia, E. D. Paula, G. R. Tofoli, and D. R. Araujo, *Mater. Sci. Eng. C*, **68**, 299 (2016).
13. H. R. R. Lin, K. C. Sung, and W. J. J. Vong, *Biomacromolecules*, **5**, 2358 (2004).
14. L. Mayol, F. Quaglia, A. Borzacchiello, L. Ambrosio, and M. I. L. Rotonda, *Eur. J. Pharm. Biopharm.*, **70**, 199 (2008).
15. T. G. Yarnykh, E. V. Tolochko, and V. N. Chushenko, *J. Pharm. Chem.*, **44**, 551 (2011).
16. H. Qi, W. Chen, C. Huang, L. Li, C. Chen, W. Li, and C. Wu, *Int. J. Pharm.*, **337**, 178 (2007).
17. I. R. Schmolka, *J. Biomed. Mater. Res.*, **6**, 571 (1972).
18. K. S. Sandhu and N. Singh, *J. Food Chem.*, **101**, 1499 (2007).
19. A. Kluk and M. Sznitowska, *Int. J. Pharm.*, **460**, 228 (2014).

20. C. Ju, J. Sun, P. Zi, X. Jin, and C. Zhan, *J. Pharm. Sci.*, **102**, 2707 (2013).

21. Q. F. Dang, J. Q. Yan, J. J. Li, X. J. Cheng, C. S. Liu, and X. G. Chen, *Carbohydr. Polym.*, **83**, 171 (2011).

22. T. Lin, J. Wu, X. Zhao, H. Lian, A. Yuan, X. Tang, S. Zhao, H. Guo, and Y. Hu, *J. Pharm. Sci.*, **103**, 927 (2014).

23. L. Mayol, M. Biondi, F. Quaglia, S. Fusco, A. Borzacchiello, L. Ambrosio, and L. Rotonda, *Biomacromolecules*, **12**, 28 (2011).

24. N. Ahuja, O. P. Katare, and B. Singh, *Eur. J. Pharm. Biopharm.*, **65**, 26 (2007).

25. S. H. Kim, S. R. Kim, H. Y. Yoon, I. H. Chang, Y. M. Whang, M. J. Cho, M. J. Kim, S. J. Lee, and Y. W. Choi, *Korean J. Urol. Oncol.*, **15**, 178 (2017).

26. D. Grennwood and F. O'Grady, *J. Antimicrob. Chemother.*, **4**, 113 (1978).

27. E. Giuliano, D. Paolino, M. Fresta, and D. Cosco, *Pharmaceutics*, **10**, 159 (2018).

28. M. Dewan, G. Sarkar, M. Bhowmik, B. Das, A. K. Chattoapadhyay, D. Rana, and D. Chattopadhyay, *Int. J. Biol. Macromol.*, **102**, 258 (2017).

29. J. M. Quintana, A. N. Califano, N. E. Zaritzky, P. Partal, and J. M. Franco, *J. Texture. Stud.*, **33**, 215 (2002).

30. J. Desbrieres, *Biomacromolecules*, **3**, 342 (2002).

31. C. M. Chang and R. Bodmeier, *Int. J. Pharm.*, **173**, 51 (1988).

32. J. Hurler, A. Engesland, B. P. Kermany, and N. S. Basnet, *J. Appl. Polym. Sci.*, **125**, 180 (2012).

33. G. Calixto, A. C. Yoshii, H. R. Silva, B. S. F. Cury, and M. Chorilli, *Pharm. Dev. Technol.*, **20**, 490 (2014).

34. H. Gupta, A. Sharma, and B. Shrivastava, *Asian J. Pharm.*, **3**, 94 (2009).

35. V. Sridhar, S. Wairkar, R. Gaud, A. Bajaj, and P. Meshram, *J. Drug. Target.*, **26**, 150 (2018).

36. A. Y. Sherif, G. M. Mahrous, and F. K. Alanazi, *Saudi Pharm. J.*, **26**, 845 (2018).

37. F. Tuğcu-Demiröz, *Marmara Pharm. J.*, **21**, 762 (2017).

38. T. Ur-Rehman, S. Tavelin, and G. Gröbner, *Int. J. Pharm.*, **409**, 19 (2011).

39. H. J. Cho, P. Balakrishnan, E. K. Park, K. W. Song, S. S. Hong, T. Y. Jang, K. S. Kim, S. J. Chung, C. K. Shim, and D. D. Kim, *J. Pharm. Sci.*, **100**, 681 (2011).

40. N. K. Sachan, S. Pushkar, A. Jha, and A. Bhattcharya, *J. Pharm. Res.*, **2**, 1191 (2009).

41. H. U. Lin, K. C. Sung, and W. J. Vong, *Biomacromolecules*, **5**, 2358 (2004).

42. M. N. Anurova, E. O. Bakhrushina, and N. B. Demia, *J. Pharm. Chem.*, **49**, 627 (2015).

43. Z. G. Yu, Z. X. Geng, T. F. Liu, and F. Jiang, *J. Vet. Pharmacol. Therap.*, **38**, 271 (2014).

44. L. Zhang, D. L. Parsons, C. Navarre, and U. B. Kompella, *J. Control. Release*, **85**, 73 (2002).

45. K. R. Lee, E. J. Kim, S. W. Seo, and H. K. Choi, *Arch. Pharm. Res.*, **31**, 1023 (2008).

46. K. Y. Cho, T. W. Chung, B. C. Kim, M. K. Kim, J. H. Lee, W. R. Wee, and C. S. Cho, *Int. J. Pharm.*, **260**, 83 (2003).

47. E. J. Strauss, J. A. Hart, M. D. Miller, R. D. Altman, and J. E. Rosen, *Am. J. Sports. Med.*, **37**, 1636 (2009).

48. L. Mayol, F. Quaglia, A. Borzacchiello, L. Ambrosio, and M. I. Rotonda, *Eur. J. Pharm. Biopharm.*, **70**, 199 (2008).

49. M. H. M. Nascimento, M. K. K. D. Franco, F. Yokaichyia, E. de Paula, C. B. Lombello, and D. R. de Araujo, *Int. J. Biol. Macromol.*, **111**, 1245 (2018).

50. N. A. Peppas and B. Narasimhan, *J. Control. Release*, **190**, 75 (2014).

51. Bruschi and M. Luciano, *Strategies to Modify the Drug Release from Pharmaceutical Systems*, Woodhead Publishing, 2015.